CHAPTER 2

Theoretical Background

This work mainly concerns about the utilization of molecular Rydberg state of Rb_2 to improve the single-atom loading efficiency in an optical trap. Since all physical phenomena related to this work happen under low temperature regime, vary from μK to mK, physics of laser cooling and trapping are important. The thermal atoms must undergo a series of cooling processes in order to reach the sufficiently low temperature such that it can be trapped in an optical trap. Section 2.1 and 2.2 give an overview of standard cooling and trapping techniques used in this thesis. Rydberg atom and its general properties are introduced in section 2.3. Section 2.4 focuses on the quantum mechanical formulation of two interacting atoms consisting of a Rydberg atom and a ground-state atom. This system plays a crucial role in development of our single-atom loading mechanism. Due to the excitation of molecular Rydberg state of Rb_2 requires two-photon transition driven by 780 nm and 480 nm light, section 2.5 gives a general description of two-photon excitation and dynamic of multilevel atom in light fields. Section 2.6 presents a theoretical model of light-assisted cold collision in blue-detuning regime. The model is used to evaluate the possibility and conditions for achieving deterministic single-atom loading.

2.1 Magneto-optical trap (MOT)

MOT is a standard technique that is widely used to cool thermal atoms from a room temperature to around hundreds of μK and confining the atoms in a particular region. The central concept of cooling atoms using MOT is that of the scattering force [19]. The origin of scattering force arise from atoms absorb photons and then momentum of photon is transferred to the atoms. For every absorbed photon, the atom receives a momentum change in the direction of photon propagation. The change of momentum due to spontaneous emission will be in random directions, hence its average change becomes zero.

Assuming an atom is a two-level system, the scattering force exerting on the atom in the presence of a laser field having wavelength of λ is given by [Ref]

$$F_{sp} = \hbar\pi\frac{\gamma}{\lambda}\left(\frac{s_o}{1+s_o+(2\Delta/\gamma)^2}\right), \tag{2.1}$$

where γ is natural decay rate, s_o is the saturation parameter, and Δ is the detuning from atomic transition. This force can be used to slow atoms by tuning frequency of laser below the transition frequency. This can be called the light is red-detuned from atomic transition. If the atom moves in a direction opposite to the beam propagation, it experience a Doppler shift that will bring the frequency of laser close to transition frequency, hence Δ is reduced and the force F_{sp} increased. The speed of atom slow down since the direction of force is opposite to the direction of atom's motion.

Spatial confinement of MOT is possible using a pair of anti-Helmhotz coils to produce a radial magnetic field gradient and three pairs of red-detuned circularly polarized, counter-propagating and counter-polarized beams. The three pairs are intersect at perpendicular angles at the point where the magnetic field is zero. Fig.(2.1) shows the illustrative optical alignment of MOT. By assuming the two-level atom has angular momentum quantum number $J = 0$ for ground state and $J = 1$ for excited state, the tapping scheme of MOT can be described as follow. Near the origin point where magnetic field is zero, the radial magnetic field $B(r)$ increases linearly, hence the Zeeman shift of sub-magnetic levels m_J are position dependent,

$$\Delta E_Z = \frac{\mu_B}{\hbar}\frac{dB}{dr}r, \tag{2.2}$$

where μ_B is the Zeeman constant and dB/dr is the magnetic field gradient in radial direction. The Zeeman shifts are shown in Fig.(2.2). It is clear that an atom moving along positive position will scatter σ^+ photons at a faster rate than σ^- photons because the Zeeman effect will shift the magnetic sub-level $m_J = +1$ down and the transition frequency closer to the light frequency (purple arrow). Consequently the atom experience imbalanced force that the net force directs to the center of trap. The same description

can be applied where the atom moves along negative position. Therefore the position dependent force acts as restoring force exerting on the atom. The total force acting on the atom is

$$F_{MOT} = -\alpha \frac{dr}{dt} - Kr, \tag{2.3}$$

where the first term on RHS is the damping force due to Doppler effect and the second term is the restoring force due to position-dependent of Zeeman effect. The damping constant α and the spring constant K are given by

$$\alpha = -4\hbar k^2 s_o \left(\frac{2\Delta/\gamma}{1 + (2\Delta/\gamma)^2} \right), \tag{2.4}$$

and

$$K = \frac{\alpha}{k} \frac{\mu_B}{\hbar} \frac{dB}{dr}, \tag{2.5}$$

where k is the wavenumber of laser.

So far the two-level system is used to describe the operation of MOT. In a real situation where atom is a multi-level atom, the excitation scheme becomes more complicated. Theoretically, cooling and trapping of rubidium-87 atoms using MOT can be achieved only via the cyclic transition $F = 2 \rightarrow F' = 3$ of the D2 line. However, the existence of non-zero line width and multi energy levels causes atom loss from the cyclic transition. Let a rubidium atom is in the hyperfine ground state $F = 2$. Although the frequency of laser may be red-detuned to fall between $F' = 2$ and $F' = 3$ so that the transition rates for $F = 2 \rightarrow F' = 1$ and $F = 2 \rightarrow F' = 2$ are small compared to $F = 2 \rightarrow F' = 3$, such small excitation rates can lead to a loss of atoms from the cooling cycle caused by spontaneous emission to the other ground state, i.e. $F' = 3 \rightarrow F = 2$. Since the splitting between the two ground states ($F = 1$ and $F = 2$ for Rubidium 87) is very large, about 6.8GHz, atoms confined in this ground state are no longer cooled and trapped. In order to survive efficient cooling and trapping, a second laser beam, called repumping beam, was used to pump atoms from the avoid ground state ($F = 1$) recaptured back to the cyclic ground state ($F = 2$).

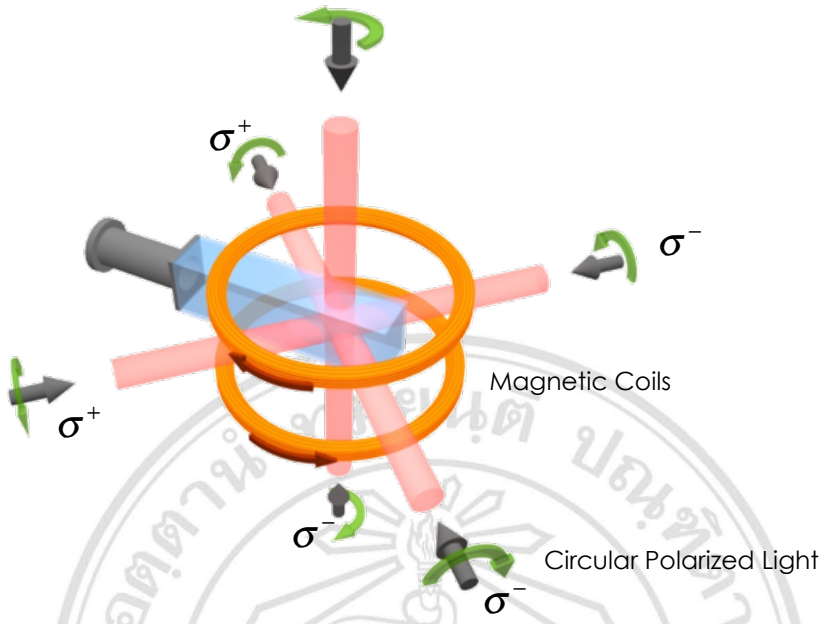

Figure 2.1: Optical alignment of magneto-optical trap.

2.2 Optical dipole trap and optical lattice

An optical dipole trap [20] confines atoms by generating the spatial gradient of energy light shift induced by a far-detuned laser light field that perturbs electronic could of an atom. The nature of dipole force is conservative and proportional to the gradient of the optical intensity. Hence it can be mathematically represented in term of a potential. The perturbation of a far-detuned laser light on a multilevel atom can be treated as a second order perturbation. The light shift of a particular state $|i\rangle$ can be written as

$$\Delta E_i = \sum_{j \neq i} \frac{|\langle j| \hat{\boldsymbol{H}}_I |i\rangle|^2}{E_i - E_j} \tag{2.6}$$

where $\hat{\boldsymbol{H}}_I$ is the interaction Hamiltonian that has the form as

$$\hat{\boldsymbol{H}}_I = \vec{\mu} \cdot \vec{E} \tag{2.7}$$

where $\vec{\mu}$ and $\vec{E}$ are dipole moment of atom and electric field of light respectively.

An illustrative picture of 1D optical lattice is shown in Fig.(2.3). The standing-

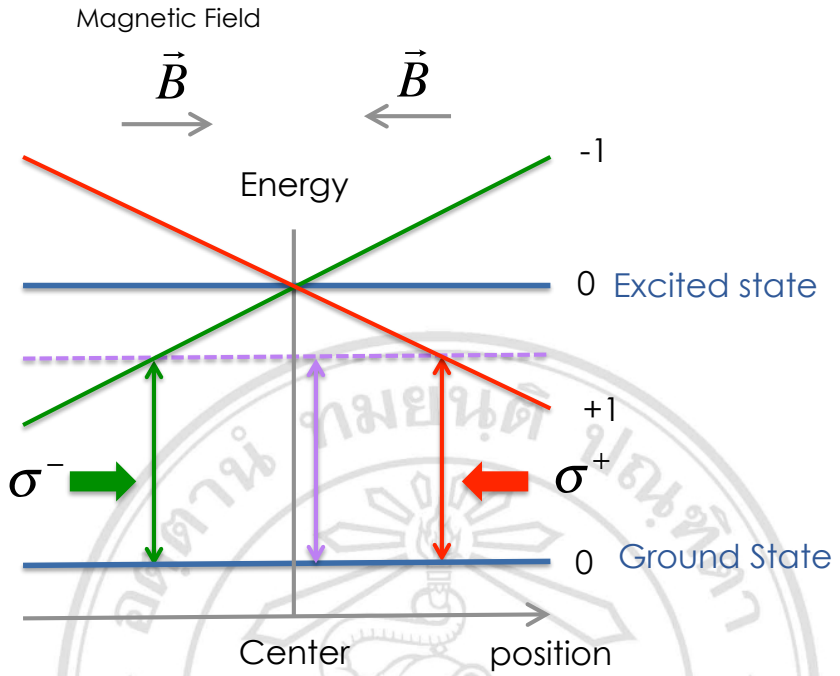

Figure 2.2: Principle of MOT

wave interference pattern creates a periodic potential inside an optical cavity formed by two cavity mirrors. Assuming TM_{00} mode where the spatial profile of the standing wave is Gaussian and letting the wavelength λ of dipole laser is very long compared to the transition wavelengths of atoms, the corresponding trap potential is written in cylindrical coordinated as,

$$U(r,\phi,z) = U_o(z)\exp\left(-\frac{2r^2}{w(z)^2}\right)\cos^2\left(\frac{2\pi}{\lambda}z\right) \tag{2.8}$$

where the trap depth $U_o(z)$ is set to be negative value and a function of position along the cavity axis $\hat{z}$. The z-dependence of U_o comes from the fact that the intensity of laser beam has different values at different position z. Here $z = 0$ means the center between the two mirrors. $w(z)$ is the beam radius of the Gaussian beam at a particular z.

2.3 Rydberg atoms

Rydberg states of an atom are defined as the electronic states that have high principle quantum number n in which its valence electron is loosely bound at a large distance from the ion core. Many behaviors and characteristics of Rydberg atoms have been

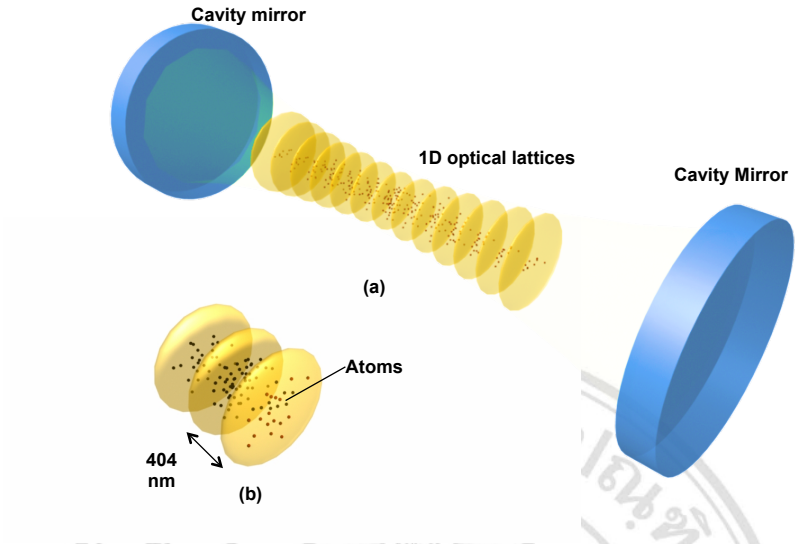

Figure 2.3: An one-dimensional optical lattice can be formed between two mirrors. Atoms are confined at anti-nodes (yellow pancake-like shape) of the standing wave. Any two adjacent sites are separated by the haft of dipole laser wavelength, here 808 nm laser is used. The picture is not drawn with true scale.

studied using the quantum defect theory [21]. General properties of Rydberg atom are very small binding energy, very long radiative lifetime [22] (vary from tens to hundreds microseconds), large dipole matrix element [23], and very sensitive to external electric field [24]. Theses atoms also exhibit strong long-range dipole-dipole interaction at distances and we proposed that it would provide deterministically a single-atom loading in an optical dipole trap.

2.3.1 Quantum Defect

According to the quantum defect theory, the energy levels of a quantum state $|n\ell j\rangle$ of an alkali atom appear as the distortion from energy levels of hydrogen atom in term of effective principle quantum number n_{eff}

$$E_{n\ell j} = -\frac{1}{2(n-\delta_{\ell j})^2} = -\frac{1}{2n_{\text{eff}}^2}, \tag{2.9}$$

Table 2.1: The quantum defect constant

Parameter	$nS_{1/2}$	$nP_{1/2}$	$nP_{3/2}$	$nD_{3/2}$	$nD_{5/2}$
δ_o	3.1311804	2.6548849	2.6416737	1.3480917	1.34646572
δ_2	0.1784	0.2900	0.2950	-0.6028	-0.5860

where n is principle quantum number and $\delta_{n\ell j}$ is called quantum defect calculated from the expression

$$\delta_{n\ell j} = \delta_o + \frac{\delta_2}{(n-\delta_o)^2}, \tag{2.10}$$

where δ_o and δ_2 are parameters obtained from fitting the measured transition energies. Mathematically, the term quantum defect δ is defined as a small defection of principle quantum number n from hydrogen atom. The origin of the defection arises from the finite size of the ionic core of the alkali atom, which for rubidium, it consists of the nucleus and 36 electrons. For low-ℓ, the valence electron penetrates into the ionic core and hence polarizes the core. The wave functions and eigenenergies of the alkali metals are modified by the interaction between nucleus and the valence electron. The experimental quantum defect constants of rubidium atom are listed in table 2.1.

2.3.2 Radiative lifetime of Rydberg states

The zero-Kelvin radiative lifetimes of Rydberg state is normally described by using a simple analytical expression of the form

$$\tau_o = \tau_R {n_{\text{eff}}}^{\epsilon} \tag{2.11}$$

where τ_R and ϵ are constants found by fitting the calculated τ_o values as a function of the effective principal quantum number n_{eff}. Values for τ_R and ϵ reported in [22] are given in table 2.2. Fig.(2.4) shows the plot of zero-Kelvin radiative lifetime of Rydberg states $nS_{1/2}$ and $nD_{3/2,5/2}$ calculated from Eq.(2.11).

Table 2.2: Values of the parameters τ_R and ϵ in Eq.(2.11)

Parameter	$nS_{1/2}$	$nP_{1/2}$	$nP_{3/2}$	$nD_{3/2}$	$nD_{5/2}$	validity range
τ_R	1.368	2.4360	2.5341	1.0761	1.0687	$10 < n < 80$
ϵ	3.0008	2.9989	3.0019	2.9898	2.9897	

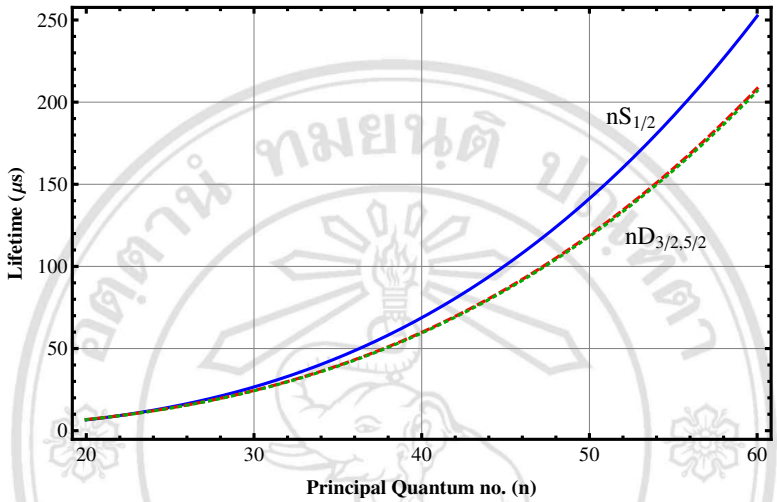

Figure 2.4: Lifetime of Rydberg state $nS_{1/2}$ (blue), $nD_{3/2}$ (dashed Red) and $nD_{5/2}$ (dotted Green) as function of principle quantum number n.

2.4 Rydberg-ground adiabatic interaction

Molecular Rydberg states play an important role in our proposed single atom loading mechanism in an optical dipole trap, section 3.1. In an experimental point of view, it is necessary to know about strength of Rydberg-ground interaction. This section presents the theoretical study of interaction between a Rydberg atom and a neutral ground-state atom. The theoretical approach and the concept of calculation method presented here follow Khuskivadze's work [25]. The adiabatic picture is exploited by assuming that relative velocity of colliding atomic pair to be much lower than velocity of Rydberg electron. This allows the application of Born-Oppenheimer approximation for the potential energy curves calculation.

Table 2.3: The fit parameters in atomic unit for the pseudopotential $V_{LS}(r)$ in Eq.(2.64) and Eq.(2.65) [25].

α	λ	State	A	γ	r_c
319.2	7.4975	^1S	4.5642	1.3438	1.8883
		^3S	68.576	9.9898	2.3813
		^1P	-4.2625	1.0055	1.8869
		^3P	-1.4523	4.8733	1.8160

2.4.1 Formalism

The system consists of a Rydberg ion core C^+, a neutral alkali ground-state atom B, and a Rydberg electron e^-, Fig. 2.5. The whole position space is divided into two hard physics regions: The region *I* where the e-B interaction (inside the sphere of radius r_0) dominated and the region *II* dominated by the e-C^+ interaction (space enclosed by surfaces S_1 and S_2). The interaction in region *I* is taken into account by utilizing the Coulomb's Green function including quantum defect [26, 27]. Due to the nature of screening effect, the e^--B interaction mainly results from the Rydberg electron interacting with the valence electron of the neutral atom B and it can be represented in term of short-range pseudopotential [28]. Hence the angular momentum basis set is chosen to be $\{L, S, J, M_J\}$ where L, S, and J are two-electron orbital angular momentum, two-electron spin, and total angular momentum respectively. Since the problem has a cylindrical symmetry along the internuclear axis $\vec{R}$, the projection of total angular momentum j on the axis is a constant of motion, hence M_J is conserved. In the Born-Oppenheimer approximation, one can consider the Hamiltonian of the Rydberg electron interacting with C^+ and B, and the Hamiltonian of C^+-B separately. For the first case, the corresponding Schrödinger equation in atomic unit of the single Rydberg electron in the presence of the neutral atom B and its ion core C^+ is

$$\left(-\frac{1}{2}\nabla^2 + \hat{V}_I(\vec{r},\vec{R}) - \frac{1}{|\vec{r}-\vec{R}|} + V_{qd}(\vec{r}-\vec{R})\right)\Phi_{M_J}(\vec{r},\vec{R}) = E_{M_J}\Phi_{M_J}(\vec{r},\vec{R}), \quad (2.12)$$

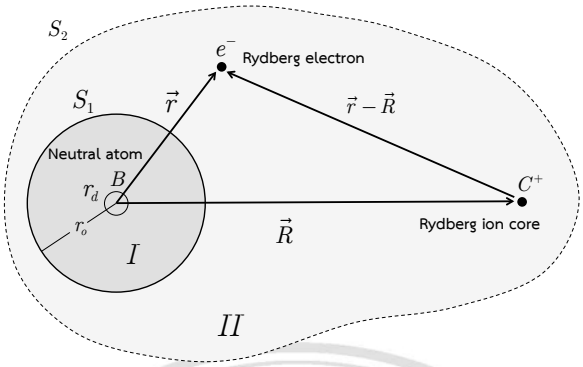

Figure 2.5: Coordinate system used in this work. The position of atom B is chosen to be the origin. The internuclear $\vec{R}$ is a vector directed form neutral atom B to the core C^+ of Rydberg atom. It is the quantization axis. $\vec{r}$ is a position vector pointed from neutral atom B to the valence electron e. r_0 is the radius of the sphere enclosed by surface S_1 dividing space into two region where the closed sufrace S_2 extends to infinity.

where the subscript M_J means that it is a good quantum number that can be used to specify an eigenstate Φ_{M_J}. The interaction potential $\hat{V}_I(\vec{r},\vec{R})$ is given by

$$\hat{V}_I(\vec{r},\vec{R}) = V_{eB}(\vec{r}) - \frac{\alpha_o \vec{r}\cdot\vec{R}}{r^3R^3}. \tag{2.13}$$

The first term of Eq.(2.13) is the combination of the spin-orbit interaction and the short-range pseudopotential of e-B that reproduces the electron binding energies for negative ion and the scattering phase shifts given by the Dirac *R*-matrix calculation [29]. The second term is the effect of three-body polarization interaction consisting of the neutral atom B polarized by the ion core C^+ interacts with the Rydberg electron e^-, and the atom B polarized by e^- interacts with the ion core C^+. The polarizability α_o of a neutral rubidium atom is given in [30]. The third and the fourth terms of Eq.(2.12) describe the Coulomb interaction and the quantum defect correction respectively. All interaction described so far are only about Rydberg electron interacting with the neutral atom and its ion core. To obtain the total energy of the interacting system C+B, it is needed to add C^+-B polarization interaction to the electron energy E_{M_J}

$$U_{M_J}(R) = E_{M_J} - \frac{\alpha_o}{2R^4}. \tag{2.14}$$

In order to find an eigenenergy of the Schrödinger equation Eq.(2.12), it is necessary to compose appropriate boundary conditions of the surface S_1 and S_2 on the Eq.(2.12) and then solve the differential equations. Due to the Coulomb interaction dominates in outer region *II* and its range is infinite, the wave function Φ_{M_J} vanishes on the surface S_2 that extends to infinity. The boundary condition on S_1 is related to the way of matching wave functions having different symmetries (spherical and cylindrical) in the two regions of space. Khuskivadze [25] have done well this matching by using the Kirchhoff-integral method in term of Coulomb Green function [31]. He matches the inner wave function with the outer wave function on the surface S_1 using the Kirchhoff integral equation. It allows him to incorporate the boundary conditions at infinity where the wave function decays exponentially. In this work, the derivation of the Kirchhoff integral equation is presented in the slightly different way. The quantum Coulomb Green's function $G_R(\vec{r},\vec{r}\,',E_{M_J})$ is defined as the solution of the Coulomb Schrödinger equation where there is a point source placed at $\vec{r}\,'$,

$$\left(-\frac{1}{2}\nabla^2-\frac{1}{|\vec{r}-\vec{R}|}+V_{qd}(\vec{r}-\vec{R})-E_{M_J}\right)G_R(\vec{r},\vec{r}\,',E_{M_J})=-\delta(\vec{r}-\vec{r}\,'), \qquad (2.15)$$

where $G_R(\vec{r},\vec{r}\,',E_{M_J})\equiv G(\vec{r}-\vec{R},\vec{r}\,'-\vec{R},E_{M_J})$ is the Green funcstion whoes center is shifted to be at $\vec{R}$. By multipying Eq. (2.12) by $G_R(\vec{r},\vec{r}\,',E_{M_J})$, Eq. (2.15) by $\Phi_{M_J}(\vec{r},\vec{R})$, then substracting one from another and take volume integration over space inside the sphere of radius r_o, the result is

$$\frac{1}{2}\int_{\mathrm{V_1}}\left(\Phi_{M_J}\nabla^2G_R-G_R\nabla^2\Phi_{M_J}\right)d^3\vec{r}+\int_{\mathrm{V_1}}\hat{V}_IG_R\Phi_{M_J}d^3\vec{r}=\Phi_{M_J}(\vec{r}\,',\vec{R}). \qquad (2.16)$$

The equation is valid if $0<r'<r_o$. After using the Green's second identity to transform the volume integral to the surface integral for the first term which contains kinetic energy operator ∇^2,

$$\frac{1}{2}\oint_{\mathrm{S_1}}\left(\Phi_{M_J}\nabla G_R-G_R\nabla\Phi_{M_J}\right)\cdot d\mathbf{S}+\int_{\mathrm{V_1}}\hat{V}_IG_R\Phi_{M_J}d^3\vec{r}=\Phi_{M_J}(\vec{r}\,',\vec{R}), \qquad (2.17)$$

where $d\mathbf{S}$ is the normal vector on S_1 and V_1 is the volume inside the sphere of radius r_o enclosed by the surface S_1. According to the scattering theory in the framework of quantum mechanics, the corresponding Lippman-Schwinger equation [32] is

$$\Phi_{M_J}(\vec{r}\,', \vec{R}) = \phi_0(\vec{r}\,', \vec{R}) + \int \hat{V}_I(\vec{r}, \vec{R}) G_R(\vec{r}, \vec{r}\,', E_{M_J}) \Phi_{M_J}(\vec{r}, \vec{R}) d^3\vec{r}, \tag{2.18}$$

where the wave function $\phi_0(\vec{r})$ is an eigenfunction of non-perturbed Rydberg atom. This eigenfunction is chosen to vanish because the system of perturbed Rydberg atom is been considering. Notice that the second term of Eq.(2.18) is the integral over all space. However if the radius r_0 is larger than the effective radius of potential $\hat{V}_I$, the infinite integral can be transformed to be a finite integral over the region inside the sphere of radius r_0. Hence, from Eq. (2.17) and Eq. (2.18),

$$\oint_{S_1} (\Phi_{M_J} \nabla G_R - G_R \nabla \Phi_{M_J}) \cdot d\mathbf{S} = 0 \qquad : 0 < r' < r_0. \tag{2.19}$$

This is the same result presented in [25,31,33] and it is called *Kirchhoff-integral equation*. It can be used as a matching condition for wave functions on the surface S_1. Hence it is an equation for determination of the eigenenergies.

In order to utilize the spirit of Eq. (2.19), it is needed to transform the integral equation into a particular form that the calculation can be performed numerically. The transformation is done by expanding Eq.(2.12) on the angular momentum basis set $|\alpha\rangle$. The short-range e-B interaction potential can be written in the form of pseudopotential as

$$\hat{V}_{eB}(\vec{r}) = \sum_{\alpha} F_\alpha(r) \left|\alpha\right\rangle \left\langle\alpha\right|, \tag{2.20}$$

where the summation is taken over angular momentum of two-electron spinor in L-S coupling scheme, $\alpha = \{L, S, J, M_J\}$. $F_\alpha(r)$ is a combination of the effective interaction of an electron and a neutral atom plus the spin-orbit interaction

$$F_{LS}(r) = V_{LS}(r) + \frac{1}{2c^2 r} \frac{dV_{LS}}{dr} (\vec{\boldsymbol{\ell}}_{\mathbf{1}} \cdot \vec{\boldsymbol{s}}_{\mathbf{1}}), \tag{2.21}$$

where $\vec{\boldsymbol{\ell}}_{\mathbf{1}} \cdot \vec{\boldsymbol{s}}_{\mathbf{1}}$ operator acts only on the Rydberg electron because it is assumed that the alkali atom B is in the ground state, hence its valence electron is in the S orbital. The pseudopotential $V_{LS}(r)$ has a spherical symmetry and its explicit form is given in subsection 2.4.3. Then the wave function $\Phi_{M_J}(\vec{R}, \vec{r})$ inside the inner region *I* is expanded in the two-electron angular momentum basis

$$\Phi_{M_J}(\vec{R}, \vec{r}) = \sum_{\alpha'} \frac{u_{\alpha'}(r)}{r} |\alpha'\rangle \,, \tag{2.22}$$

where $u_{\alpha'}(r)$ is the *radial* wave function and the angular momentum basis $|\alpha\rangle$ is expanded on the uncouple basis $|LM_L\rangle$ and $|SM_S\rangle$

$$|\alpha\rangle = |LSJM_J\rangle = \sum_{M_L, M_S} C^{J,M_J}_{L,M_L,S,M_S} |LM_L\rangle |SM_S\rangle \,, \tag{2.23}$$

where $\vec{\boldsymbol{L}} = \vec{\boldsymbol{\ell}}_{\mathbf{1}} + \vec{\boldsymbol{\ell}}_{\mathbf{2}}$, and $\vec{\boldsymbol{S}} = \vec{\boldsymbol{s}}_{\mathbf{1}} + \vec{\boldsymbol{s}}_{\mathbf{2}}$ are total orbital angular momentum and total spin of two electron. The Clebsch-Gordan coefficients C^{J,M_J}_{L,M_L,S,M_S} are given by,

$$C^{J,M_J}_{L,M_L,S,M_S} = (-1)^{-L+S-M_J} \sqrt{2J+1} \begin{pmatrix} L & S & J \\ M_L & M_S & -M_J \end{pmatrix} , \tag{2.24}$$

where $|LM_L\rangle$ are the spherical harmonics, and $|SM_S\rangle$ are the total spin states of the Rydberg electron and the valence electron. After substituting Eq. (2.22) into Eq. (2.12), neglecting the quantum defect V_{qd} due to the effect is very small in the inner region, and then projecting Eq. (2.12) on $\langle\alpha|$, the result is the system of coupled second-order differential equations

$$\left(-\frac{1}{2}\frac{d^2}{dr^2} + \frac{L(L+1)}{2r^2} + V_{LS}(r) + I_\alpha(r) - E_{M_J} \right) u_\alpha(r, R) = \sum_{\alpha'} D_{\alpha\alpha'} u_{\alpha'}(r, R), \tag{2.25}$$

where

$$D_{\alpha\alpha'} = \langle LSJM_J | \frac{1}{|\vec{r} - \vec{R}|} + \frac{\alpha_o \vec{r} \cdot \vec{R}}{r^3 R^3} |L'S'J'M_J\rangle \,, \tag{2.26}$$

and

$$I_\alpha(r) = \frac{1}{2c^2 r}\frac{dV_{LS}}{dr}\left\langle LSJM_J\right|\vec{\boldsymbol{\ell}}_{\mathbf{1}}\cdot\vec{\boldsymbol{s}}_{\mathbf{1}}\left|LSJM_J\right\rangle. \tag{2.27}$$

Using Eq. (2.23) and the expansion

$$\frac{1}{|\vec{r}-\vec{R}|} = \sum_{\ell=0}^{\infty}\sum_{m=-\ell}^{\ell}\frac{r_<^\ell}{r_>^{\ell+1}}\left(\frac{4\pi}{2\ell+1}\right)Y^*_{\ell m}(\hat{\boldsymbol{r}})Y_{\ell m}(\hat{\boldsymbol{R}}), \tag{2.28}$$

where z axis is chosen along internuclear axis $\vec{R}$ and due to considering in the inner region it can be set $r < R$, hence

$$\frac{1}{|\vec{r}-\vec{R}|} = \sum_{\ell=0}^{\infty}\frac{r^\ell}{R^{\ell+1}}\sqrt{\frac{4\pi}{2\ell+1}}\,Y_{\ell 0}(\hat{\boldsymbol{r}}), \tag{2.29}$$

and then the matrix element Eq. (2.26) becomes

$$\begin{aligned} D_{\alpha\alpha'} = \delta_{SS'}(-1)^{-L-L'}&\sqrt{(2J+1)(2J'+1)(2L+1)(2L'+1)} \\ &\times\sum_{\ell=|L-L'|}^{|L+L'|}\left(\frac{r^\ell}{R^{\ell+1}}+\frac{\alpha_d}{r^2R^2}\delta_{\ell 1}\right)\begin{pmatrix} L & \ell & L' \\ 0 & 0 & 0\end{pmatrix}B^\ell_{\alpha\alpha'} \end{aligned} \tag{2.30}$$

and

$$B^\ell_{\alpha\alpha'} = \sum_{M_L,M_S}^{M_L+M_S=M_J}(-1)^{M_L}\begin{pmatrix} L & S & J \\ M_L & M_S & -M_J\end{pmatrix}\begin{pmatrix} L & \ell & L' \\ -M_L & 0 & M_L\end{pmatrix}\begin{pmatrix} L' & S' & J' \\ M_L & M_S & -M_J\end{pmatrix} \tag{2.31}$$

where the symbols in parenthesis denote *3j* symbol coefficients. Eq.(2.25) is the coupled radial Schrödinger equation and it can be solved numerically using a standard method in electron-atom collision theory. To solve the equations, the set of linearly independent solutions needed to be calculated first and then by exploiting the boundary condition Eq.(2.19), a suitable combination of linearly independent solutions and an eigenenergy are determined. Mathematically, a general solution of the radial Schrödinger equation Eq.(2.25) consists of regular and irregular solutions at origin. However, a physical solution should be only written as a summation of linearly independent solutions regular at

origin

$$u_{\alpha'}(r,R) = \sum_j A_j \nu_{\alpha' j}(r,R), \tag{2.32}$$

where j denotes independent solutions, and A_j are constants. The matrix $\nu_{\alpha' j}$ is called *fundamental matrix* for Eq.(2.25). Note that the number of linearly independent solutions regular at origin is equal to the number of coupled differential equations. After substituting Eq.(2.22) and Eq.(2.32) into Eq.(2.19) and then projecting on $\langle\alpha|$,

$$\sum_j A_j K_{\alpha j}(E_{M_J}) = 0, \tag{2.33}$$

where

$$K_{\alpha j}(E_{M_J}) = \sum_{\alpha'} \delta_{SS'} \tag{2.34}$$

However, near the origin, the spin-orbit interaction has non-physical singularity. the Dirac equation must be applied near the origin and then calculated Dirac wave function is transformed into Schrödinger wave function in jj representation and then transform it into LS representation (Appendix B) before performing numerical integration. This process, naturally, must be repeated for varying values of the internuclear separation R in order to map out the internuclear potentials.

2.4.2 Coulomb Green function and quantum defect correction

This section presents the expression and numerical estimation of Coulomb Green's function. Consider definition of the Coulomb Green function $G(\vec{r}_1, \vec{r}_2, E)$ as,

$$\left(-\frac{1}{2}\nabla_1^2 - \frac{1}{r_1} + V_{qd}(r_1) - E\right) G(\vec{r}_1, \vec{r}_2, E) = -\delta(\vec{r}_1 - \vec{r}_2) \tag{2.35}$$

Mathematically, the solution of Eq. (2.35) can be written as in the form of an eigenfunction expansion.

$$G(\vec{r}_1, \vec{r}_2, E) = -\sum_{\ell=0}^{\infty}\sum_{m=-\ell}^{\ell}\int_0^{\infty} \frac{\phi^*_{\ell m}(k,\vec{r}_1)\phi_{\ell m}(k,\vec{r}_2)}{(k^2/2) - E} dk - \sum_{n=0}^{\infty}\sum_{\ell=0}^{\infty}\sum_{m=-\ell}^{\ell} \frac{\phi^*_{n\ell m}(\vec{r}_1)\phi_{n\ell m}(\vec{r}_2)}{E_n - E} \tag{2.36}$$

The first term is the summation and integration over the continuous spectrum of hydrogen atom. The second term is summed over the discrete spectrum. In order to include the quantum defect in calculation, the Green function $G(\vec{r}_a, \vec{r}_b, \nu)$ has two components as

$$G(\vec{r}_1, \vec{r}_2, \nu) = G_o(\vec{r}_1, \vec{r}_2, \nu) + G_{qd}(\vec{r}_1, \vec{r}_2, \nu) \tag{2.37}$$

The first term is the particular solution of inhomogeneous equation Eq. (2.35) and the second term is the solution of homogeneous equation. The *effective quantum number* v is defined by

$$\nu \equiv \frac{1}{\sqrt{-2E}} \tag{2.38}$$

The pure Coulomb Green function in closed form is given by

$$G_o(\vec{r}_1, \vec{r}_2, \nu) = -\frac{\Gamma(1-\nu)}{2\pi|\vec{r}_1 - \vec{r}_2|}\left[W_{\nu,1/2}(\alpha)\frac{\partial}{\partial\beta}M_{\nu,1/2}(\beta) - M_{\nu,1/2}(\beta)\frac{\partial}{\partial\alpha}W_{\nu,1/2}(\alpha)\right] \tag{2.39}$$

where

$$\frac{\partial}{\partial\beta}M_{\nu,1/2}(\beta) = \left(\frac{1}{2} - \frac{\nu}{\beta}\right)M_{\nu,1/2}(\beta) + \left(\frac{1+\nu}{\beta}\right)M_{1+\nu,1/2}(\beta) \tag{2.40}$$

$$\frac{\partial}{\partial\alpha}W_{\nu,1/2}(\alpha) = \left(\frac{1}{2} - \frac{\nu}{\alpha}\right)W_{\nu,1/2}(\alpha) - \frac{1}{\alpha}W_{1+\nu,1/2}(\alpha) \tag{2.41}$$

and the arguments α and β are defined as

$$\alpha \equiv \frac{1}{\nu}\left(|\vec{r}_1| + |\vec{r}_2| + |\vec{r}_1 - \vec{r}_2|\right) \tag{2.42}$$

$$\beta \equiv \frac{1}{\nu}\left(|\vec{r}_1| + |\vec{r}_2| - |\vec{r}_1 - \vec{r}_2|\right) \tag{2.43}$$

Note that $M_{k,m}(z)$ and $W_{k,m}(z)$ are *Whittaker* function of first kind and second kind respectively. They are defined as

$$M_{k,m}(z) = e^{-z/2}z^{m+1/2}{}_1\boldsymbol{F}_1(\frac{1}{2} + m - k, 1 + 2m; z) \tag{2.44}$$

$$W_{k,m}(z) = e^{-z/2}z^{m+1/2}\boldsymbol{U}(\frac{1}{2} + m - k, 1 + 2m; z) \tag{2.45}$$

where ${}_1\boldsymbol{F_1}$ and $\boldsymbol{U}$ are *confluent hypergeometric functions* of first kind and second kind. The quantum defect correction of Green function is given by

$$\begin{aligned} G_{qd}(\vec{r}_1,\vec{r}_2,\nu) = -\frac{\nu}{r_1 r_2}\sum_{\ell=0}^{\infty}\frac{\Gamma(1+\ell-\nu)}{\Gamma(1+\ell+\nu)}\frac{sin[\pi(\delta_\ell+\ell)]}{sin[\pi(\delta_\ell+\nu)]}\frac{2\ell+1}{4\pi}P_\ell(cos\gamma) \\ \times W_{\nu,\ell+1/2}\left(\frac{2r_1}{\nu}\right)W_{\nu,\ell+1/2}\left(\frac{2r_2}{\nu}\right) \end{aligned} \tag{2.46}$$

where γ is the angle between $\vec{r}_1$ and $\vec{r}_2$, and δ_ℓ is the ℓ dependent quantum defects. It should be noted that by combining the Coulomb Green function and the quantum defect correction the Coulomb poles in the sum Eq. (2.37) cancel out exactly. The remaining poles are determined by

$$E_{n\ell} = -\frac{1}{2(n-\delta_\ell)^2} \tag{2.47}$$

Let the coordinate system be defined as following,

$$\begin{aligned} \vec{r}_1 &\equiv \vec{r}_a - \vec{R} \\ \vec{r}_2 &\equiv \vec{r}_b - \vec{R} \end{aligned} \tag{2.48}$$

where the vector $\vec{R}$ is directed from the neutral atom to the Coulomb ion core. Hence the cosine of angle between $\vec{r}_a - \vec{R}$ and $\vec{r}_b - \vec{R}$ is given by

$$cos\gamma = \frac{(\vec{r}_a - \vec{R})\cdot(\vec{r}_b - \vec{R})}{|\vec{r}_a - \vec{R}||\vec{r}_b - \vec{R}|} \tag{2.49}$$

The matrix element of the Green function $\langle LM_L|\, G_R\, |L'M_L\rangle$ is

$$\langle LM_L|\, G_R\, |L'M_L\rangle \equiv A\int_{S_b}\int_{S_a} Y^*_{L,M_L}(\hat{\Omega}_a)G_R(\vec{r}_a,\vec{r}_b,\nu)Y_{L',M_L}(\hat{\Omega}_b)d\Omega_a d\Omega_b \tag{2.50}$$

where the subscript R denotes R-dependence of the matrix element and the constant A is

$$A = \sqrt{\frac{(2L+1)}{4\pi}\frac{(L-|M_L|)!}{(L+|M_L|)!}} \times \sqrt{\frac{(2L'+1)}{4\pi}\frac{(L'-|M_L|)!}{(L'+|M_L|)!}} \tag{2.51}$$

Due to the cylindrical symmetry, the four dimensional integration can be reduced to three dimensional integration. Letting $r_b \sim r_a = r_0$, we obtain

$$\begin{aligned}\langle LM_L|\, G_o\, |L'M_L\rangle = -A\Gamma(1-\nu)\int_0^{2\pi}\int_0^{\pi}\int_0^{\pi}\Bigg[\nu\left(\frac{1}{\alpha}-\frac{1}{\beta}\right)W_{\nu,1/2}(\alpha)M_{\nu,1/2}(\beta) \\ + \left(\frac{1+\nu}{\beta}\right)M_{1+\nu,1/2}(\beta)W_{\nu,1/2}(\alpha) \\ + \left(\frac{1}{\alpha}\right)W_{1+\nu,1/2}(\alpha)M_{\nu,1/2}(\beta)\Bigg] \\ \times \frac{P_{L'}^{|M_L|}(cos\theta_a)P_L^{|M_L|}(cos\theta_b)}{|\vec{r}_a-\vec{r}_b|}e^{iM_L\phi}sin\theta_a sin\theta_b \boldsymbol{d}\theta_a \boldsymbol{d}\theta_b \boldsymbol{d}\phi\end{aligned} \tag{2.52}$$

where α and β in this coordinate system are given by,

$$\alpha(\theta_a,\theta_b,\phi) = \frac{1}{\nu}\left(|\vec{r}_a-\vec{R}|+|\vec{r}_b-\vec{R}|+|\vec{r}_a-\vec{r}_b|\right) \tag{2.53}$$

$$\beta(\theta_a,\theta_b,\phi) = \frac{1}{\nu}\left(|\vec{r}_a-\vec{R}|+|\vec{r}_b-\vec{R}|-|\vec{r}_a-\vec{r}_b|\right) \tag{2.54}$$

where

$$|\vec{r}_a-\vec{R}| = r(\theta_a) \tag{2.55}$$

$$|\vec{r}_b-\vec{R}| = r(\theta_b) \tag{2.56}$$

$$|\vec{r}_a-\vec{r}_b| = \sqrt{2}r_0\sqrt{1-cos\gamma} \tag{2.57}$$

where $r(\theta) \equiv \sqrt{r_0^2+R^2-2r_0Rcos\theta}$. The cosine of angle γ is given by

$$cos\gamma = C(\theta_a,\theta_b)cos\phi + D(\theta_a,\theta_b) \tag{2.58}$$

where

$$C(\theta_a,\theta_b) = \frac{r_0^2 sin\theta_a sin\theta_b}{r(\theta_a)r(\theta_b)} \tag{2.59}$$

$$D(\theta_a,\theta_b) = \frac{(r_0cos\theta_a - R)(r_0cos\theta_b - R)}{r(\theta_a)r(\theta_b)} \tag{2.60}$$

For the quantum defect correction,

$$\begin{aligned}\langle LM_L|\, G_{qd}\, |L'M_L\rangle = 2\pi A\nu \sum_{\ell=0}^{5} \frac{\Gamma(1+\ell-\nu)}{\Gamma(1+\ell+\nu)} \frac{sin[\pi(\delta_\ell+\ell)]}{sin[\pi(\delta_\ell+\nu)]} \frac{2\ell+1}{4\pi} \\ \times \int_0^\pi \int_0^\pi \frac{W_{\nu,\ell+1/2}\left(\frac{2r(\theta_a)}{\nu}\right) W_{\nu,\ell+1/2}\left(\frac{2r(\theta_b)}{\nu}\right)}{r(\theta_a)r(\theta_b)} F_{\ell,M_L}(\theta_a,\theta_b) \\ \times P_{L'}^{|M_L|}(cos\theta_a) P_L^{|M_L|}(cos\theta_b) sin\theta_a sin\theta_b \boldsymbol{d}\theta_a \boldsymbol{d}\theta_b\end{aligned} \tag{2.61}$$

where $P_L^M(z)$ is the *associated Legendre* polynomial (see *Introduction to Quantum mechanics, Davis J. Griffith, 2rd edition, p136*). The summation over ℓ in quantum defect correction is limited to the first five terms because the quantum defects for high ℓ can be ignored. The functions $F_{\ell,M_L}(\theta_a,\theta_b)$ is given by

$$F_{\ell,M_L}(\theta_a,\theta_b) = \int_0^{2\pi} P_\ell(cos\gamma) e^{iM_L\phi_a} d\phi \tag{2.62}$$

where $P_\ell(z)$ is the *Legendre* polynomial.

In order to remove poles of Green function for zero searching calculation, the matrix element can be multiplied by

$$\frac{\prod_{\ell=0}^{5} sin[\pi(\delta_\ell+\nu)]}{\Gamma(1-\nu)} \tag{2.63}$$

2.4.3 Effective interaction for electron-atom scattering

The method used to describe the interaction between an electron and an alkali atom in low-energy scattering scheme is the model-potential approach [28, 34]. Due to scattering energy is low, it is naturally to ignore the scattering wave with $L > 1$ hence only s and p wave scattering are relevant. It should be noted that by separating the interaction potentials with different orbital angular momentum L, the effective interaction can be called pseudopotential. The model-potential $V_{LS}(r)$ in Eq.(2.21) for s-wave scattering, $L = 0$, has an analytic form in atomic unit as

$$V_{0S}(r) = -\frac{A}{r}e^{-\gamma r} - \frac{\alpha}{2r^4}\left(1 - e^{(r/r_c)^6}\right) \tag{2.64}$$

while for the p-wave scattering, $L = 1$, the potential is written as

$$V_{1S}(r) = -\frac{Z_c}{r}e^{-\lambda r} - Ae^{-\gamma r} - \frac{\alpha}{2r^4}\left(1 - e^{(r/r_c)^6}\right) \tag{2.65}$$

where the constants A, γ, α, and λ are fitted parameters shown in Table.2.3. Z_c is the nuclear charge, for rubidium atom it is 37. Physics of scattering between low-energy electron and an alkali atom is relevant to a virtual ^3S state and a ^3P shape resonance [35, 36]. These features play an important role in formation of long-range molecular Rydberg states. The classical description of a shape resonance in scattering is presented [37] by the projectile of incoming electron tunneling through a potential barrier due to repulsive electron-electron interaction. The electron remains within a pseudo-bound state for a while and then tunneling out from the barrier. Although there is no a classical description of a virtual state in scattering, a simple picture of the state is described as follow. As the depth of an attractive scattering potential is decreased provided there is no potential barrier, an energy level of a bound state moves through the continuum threshold to become a pseudo-bound state called virtual state [38].

2.5 Multi-level atom in light fields and two-photon transition

The semi-classical Hamiltonian of a system consisting of an multi-level atom interacting with coherent electromagnetic fields is

$$\begin{aligned}\hat{H} &= \hat{H}_0 + \hat{V}_I(t) \\ &= \sum_j E_j \left|j\right\rangle \left\langle j\right| - \sum_{i\neq j,k} \vec{\mu}_{ij} \cdot \vec{\boldsymbol{E}}_k \left|i\right\rangle \left\langle j\right|\end{aligned} \tag{2.66}$$

where the $\hat{H}_0$ denotes the field-free time-independent atomic Hamiltonian whose eigenvalues and eigenfunctions are $E_\alpha = \hbar\omega_\alpha$ and $|\alpha\rangle$ respectively. The second term, $\hat{H}_I$, is the time-dependent interaction with radiation fields of mode k. This interaction plays the important role in transition between eigenstates of atomic Hamiltonian $\hat{H}_0$. The time evolution of optical transition of multi-level atom in the presence of coherent light fields is described using the density matrix formulation. The density operator $\hat{\rho}$ of a multi-level

system in a pure state $|\Psi\rangle$ is given by

$$\hat{\rho}(t) = |\Psi(t)\rangle \langle\Psi(t)| , \tag{2.67}$$

where the state $|\Psi(t)\rangle$ can be written in the interaction picture [32] as superposition of all eigenstates of the unperturbed Hamiltonian $\hat{H}_0$.

$$|\Psi(t)\rangle = \sum_{\alpha} C_{\alpha}(t) |\alpha\rangle . \tag{2.68}$$

The evolution of the density operator $\hat{\rho}$ in the representation is then described by a system of equations known as the optical Bloch equations.

$$\frac{d\hat{\rho}}{dt} = \frac{i}{\hbar}\left[\hat{\rho}, \hat{V}_I(t)\right] + \hat{G}(\gamma, \hat{\rho}), \tag{2.69}$$

where $\hat{G}$ is the operator accounting for the relaxation effect due to decoherence processes. Applying the standard *rotating wave approximation*, the matrix element of interaction potential is

$$V_{ij} = \sum_{k} \hbar \frac{\Omega_{ij}^{k}}{2} e^{-i\Delta_{ij}^{k} t}, \tag{2.70}$$

where Ω_{ij}^{k} is the on-resonance ***Rabi frequency*** of atomic transition $i \rightarrow j$ driven by the radiation field of mode k. This frequency fundamentally represents how fast atom absorbs photon and reemit the photon via stimulated absorption and stimulated emission. The detuning $\Delta_{ij}^{k} = \omega_k - \omega_{ij}$ is the frequency difference between the radiation field of mode k and the transition ij.

The operator $\hat{G}$ has both diagonal and off-diagonal (coherence) elements. Assuming that all decoherence arise from the spontaneous emission. Then the diagonal elements are determined from the conservation of probability and the off-diagonal elements G_{ij} are proportional to only the spontaneous emission rate γ_{ij} of decay channel $i \rightarrow j$. The rate γ_{ij} is determined by considering the interaction of an atom with quantized electromagnetic field in free space. This phenomena corresponds with a discrete level system

coupled to a continuum states of external field. The interaction Hamiltonian is given by

$$\hat{H}_I = i \sum_k \sum_{i \neq j} \left(\frac{\hbar \omega_k}{2 \epsilon_o V} \right)^{1/2} \mu_{ij} \cdot \vec{E}_k \left[\hat{a}_k e^{i(\vec{k} \cdot \vec{r} - \omega_k t)} - \hat{a}_k^\dagger e^{-i(\vec{k} \cdot \vec{r} - \omega_k t)} \right] |i\rangle \langle j| \qquad (2.71)$$

where the summations are taken over both all field modes k and atomic transitions of interest $i \rightarrow j$. When the analytic expression of $\hat{G}$ is known, the Eq.(2.69) can be used to setup the master equations where its solutions describe the dynamic picture of a multi-level atom in multi-mode radiation fields. Appendix C presents the application of the formulation in quantum dynamic of magneto-optical trap.

2.5.1 Two-photon transition

Fundamentally a transition frequency from a ground-state to a Rydberg state of an alkali atom is in an order of hundreds THz. There is no available laser having corresponding wavelength to do single-photon excitation. Hence in many Rydberg experiments the two-photon excitation is used. Dynamic of two-photon transition can be studied through a three-level system interacting with two laser fields. In Rydberg case, the system forms a ladder in which successive energies lie higher than the predecessor. The laser field coupling the ground state to the intermediate state is called *probe beam* and the other field, called *coupling beam* couples the intermediate state and the Rydberg state.

2.6 Light-assisted cold collision in blue-detuning regime

This section presents the general concept of light-assisted collision in blue detuning scheme. Landau-Zener formula used in calculation probability of inelastic collision and the physics of two-photon transition.

2.6.1 Landau-Zener model

This section presents semiclassical picture used for describing cold collision in light field. The The Landau-Zener probability that the collision partner remain on the ground

state as it passes once through the interaction region is,

$$P_g = \exp\left(-\frac{\pi\hbar\Omega^2}{2\alpha|p|/\mu}\right) \tag{2.72}$$

where Ω is the Rabi frequency and α is the slope of the difference potential $U(R) = U_e(R) - U_g(R)$ evaluated at the Condon point R_c,

$$\alpha = \left|\frac{d\Delta}{dR}\right|_{R_c} = \left.\frac{dU(R)}{dR}\right|_{R_c} \tag{2.73}$$

The parameter μ is the reduced mass of collision partner. The momentum p is given by the relation to kinetic energy at a particular temperature T.

$$E_{kin} = \frac{p^2}{2\mu} \equiv k_B T \tag{2.74}$$

The probability of exiting the collision on the excited state asymptote after traversing the crossing region twice is

$$P_e^{\infty} = P_g(1 - P_g) \tag{2.75}$$